Metallurgy and materials
Metalurgia e materiais

Effects of the addition of graphene on the compressive strength of geopolymeric mortar developed from k-feldspar mining waste

http://dx.doi.org/10.1590/0370-44672020740138

Vinícius Meirelles Mendonça[1,2,3]
https://orcid.org/0000-0002-1817-168X
Flávio Renato de Góes Padula[1,4]
https://orcid.org/0000-0002-7166-8433
Sidney Nicodemos Silva[1,5]
https://orcid.org/0000-0002-4431-6651
Plínio Fernandes Borges Silva[1,6]
https://orcid.org/0000-0001-8862-0041
Jefferson de Paula[1,7]
https://orcid.org/0000-0002-1531-1552

[1]Centro Federal de Educação Tecnológica de Minas Gerais – CEFET-MG, Departamento de Engenharia de Materiais, Belo Horizonte – Minas Gerais - Brasil.

[2]Centro de Tecnologias Estratégicas do Nordeste - CETENE, Recife - Pernambuco – Brasil.

E-mails: [3]viniciusmeirelles41@hotmail.com, [4]padula@cefetmg.br, [5]sidney.nicodemos@yahoo.com.br, [6]plinio.eng1707@gmail.com, [7]jeffpaula@hotmail.com

Abstract

Contemporary organizations are showing a growing interest in the reuse of solid waste from industrial processes with the intention of reducing environmental impacts and reducing costs. The mining activity is one of the main waste generators in Brazil. In parallel, geopolymeric materials have been gaining prominence in studies that make it a possible substitute for ordinary Portland cement, due to its environmental advantages. Therefore, the present research proposes to study the feasibility of using K-feldspar mining waste as a possible raw material for the manufacture of geopolymer cements. In addition, in line with the latest technological trends, the addition of multi-layered graphene was evaluated as a structural reinforcement for geopolymeric mortar. Graphene was added in three percentages: 0.1 wt.%, 0.3 wt.% and 0.5 wt.%. Specimens were produced in order to evaluate the compressive strength of these materials. As a complementary characterization, the analysis of EDX, laser diffraction particle size and XRD of the waste were performed, as well as SEM and TEM analysis of the graphene used. The results showed that the geopolimerization was effective and that the 0.5% graphene content promoted a significant increase of 65% in the compressive strength. It is concluded, therefore, that with the achieved mechanical strength values, the studied waste can be applied as mortar in auxiliary structures using the geopolymerization technique and that graphene can be used to promote increases in the mechanical strength of the material produced.

Keywords: graphene, geopolymers, waste.

1. Introduction

Social responsibility and sustainability have become constant concerns in the current world geopolitical scenario. Thus, organizations are developing measures to evaluate environmental performance and investing in sustainable practices in order to increase medium to long term gains (Gomes, 2017).

The mining industry plays a prominent role in this scenario, and according to Araújo *et. al* (2012), it is an indispensable sector for the country's economy, being the foundation of the production chain, since the products generated by mining operations are present in the daily life of society in a significant and substantial way. However, with the exception of its relevance, mining has the ability to provide numerous negative environmental impacts.

The waste generated by mining processes has been responsible for numerous environmental impacts, making it a target for studies aiming to reuse this material (Gomes, 2017). From 1996 to 2005, mining waste generation increased from 202 million tons to 290 million tons in 2005, an increase of 1.4 times.

Meanwhile, the need to reduce energy consumption and CO_2 emissions is a constant requirement for the Portland Cement industry, forcing the improvement of manufacturing process efficiency as well as the reusing of waste and by-products from other industries (Yun-Ming *et al*., 2016). Geopolymer cements appear as a new class of high-performance materials for structural applications being a mineral binder capable of totally or partially replacing Portland Cement (Turner and Collins, 2013; Mehta and Siddique, 2016).

Finally, graphene can be extracted from graphite through a process known as chemical exfoliation and is extremely light and resistant. When used as a filler in composites, it is possible to achieve higher strengths. It has excellent mechanical, chemical, electrical, thermal and optical properties. It is a great conductor of heat and electricity and chemically reacts well when mixed with other materials (Yan *et al.*, 2015).

The main purpose of this study was to investigate a possibility of reusing the k-feldspar extraction waste for the manufacture of geopolymers and then adding graphene to the material produced in order to promote an increase in its mechanical strength.

2. Materials and methods

Initially, the chemical analysis of the K-feldspar extraction tailings was performed in a Shimadzu EDX-720® in order to identify and quantify the present oxides. The tests were performed with powder samples, after drying, arranged in a sample holder and covered with TF-250 Polypropylene Film. A vacuum atmosphere was used. The purpose of this test was to identify the oxides present and their concentrations.

The laser diffraction particle size test using the CILAS 1190® was performed to measure the particle size distribution of the waste and X-ray diffraction was done in the Shimadzu XRD6000® to determine the present phases. Measurements were made in an aqueous medium with an obscurity value of approximately 15%, using 60 seconds of ultrasound and using the Fraunhofer model.

X-ray diffraction tests were performed to detect the phases present in the K-feldspar waste and compare with the phases identified in the samples after geopolimerization, in particular the samples with 0 wt.%; 0.1 wt.%; 0.3 wt.% and 0.5 wt.% graphene. The scan angle used was $5° < 2\theta < 80°$, with a scan speed of 2° / min and a copper target was used.

For the study of graphene, we used a scanning electron microscopy (SEM) technique in SEM TESCAN® Vega 3. A voltage of 30kV was used in Tungsten filament. The image was taken at magnification of 32,000 times with secondary electron detector, in order to assess the morphology and aspects of the graphene layers.

For further visualization of graphene morphology, images were made in the Transmission Electron Microscope (TEM) JEOL®JEM 2100. Operated with LaB6 cathode at 200 kV. A drop of a powder immersion in 2 propanol was placed on a holey carbon coated copper TEM grid (model S1474, supplied by Plano®), and dried in air before investigation.

The K-feldspar waste was sieved through a 5mm sieve and dried in a muffle oven at 120°C for 3 hours before it could be subjected to the geopolymerization reaction.

Mixtures were made by adding 2 wt.% and 4 wt.% respectively of sodium hydroxide and sodium silicate as activating solutions. The Alkaline sodium silicate (type C-122, 14.8% Na_2O) was supplied by Phosther Tecnologia de Aglomerações® and sodium hydroxide (50% aqueous solution) supplied by Sulfal Química Ltda®.

Graphene was supplied as a powder, presenting 99.94% purity, by the company Phosther Tecnologia de Aglomerações®, which developed a multilayer graphene synthesis method that allows it to obtain lower production costs and allowing selling prices compatible with the cement market. The material presents a 99.94% purity, and a heterogeneous structure that varies from 30 to 50 layers. Mendonça (2020) presents a further characterization of this product.

Graphene was added in three proportions: 0.1 wt.% (sample G0.1); 0.3 wt.% (G0.3 sample) and 0.5 wt.% (G0.5 sample) and G0 sample as reference sample without graphene reinforcement.

After mixing, specimens were prepared according to the ABNT NBR 16697:2018 standard for Portland CP-II cement. As there is a shortage of standards for geopolymeric materials, a standard for Portland cement was used, which is, a priori, the material that geopolymers are intended to partially replace.

The samples were pressed in a hydraulic press with a load of approximately 9 tons, generating specimens of 10 cm height x 5 cm diameter. The materials were cured at 80°C for 720 minutes (12 hours). Yun-Ming *et al.* (2016) states that the temperature used for curing geopolymers should be between 20 ° C and 100 ° C in order to allow a correct geopolymerization reaction. Arioz, Arioz and Koçkar (2014) mentions that the increase in both curing temperature and curing time allows the obtaining of geopolymers with greater compressive strength, considering that for times longer than 15 hours, he did not obtain any strength improvement.

The specimens were tested according to the ABNT NBR 16697:2018 standard to determine the maximum compressive strength value.

3. Results

X - ray fluorescence analysis results of the waste can be seen in Table 1. The values are presented in wt.%.

Table 1 – Oxide concentration in waste sample.

Oxides	Weight (wt.%)
Al_2O_3	51.2
SiO_2	36.6
K_2O	7.8
MgO	3.1
Fe_2O_3	1.3

Laser diffraction particle size analysis for the K-feldspar waste results can be seen in Table 2. D10, D50 and D90 correspond to the total of diameters at 10%, 50% and 90% of the sample. D-average corresponds to the average particle size of the material. Fig. 1 presents the histogram obtained in the same laser diffraction particle size analysis, showing the particle size distribution of the sample.

Table 2 – Particle size values of the K-Felspar waste.

Diameters	Values (μm)
D10	2.99
D50	8.60
D90	17.85
D-average	9.65

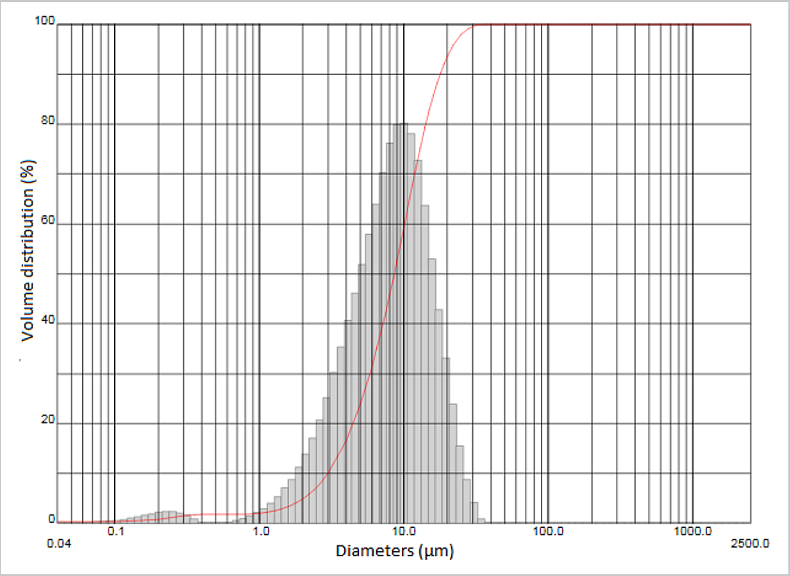

Figure 1 – Particle size distribution of the K-Feldspar waste.

X-ray diffraction test of the waste sample is shown in Fig.2. The following five phases were identified in the gray waste: muscovite, quartz, orthoclase, albite and kaolinite. The respective cards in the ICDD database are: 841305, 861628, 860439, 832215 and 751593.

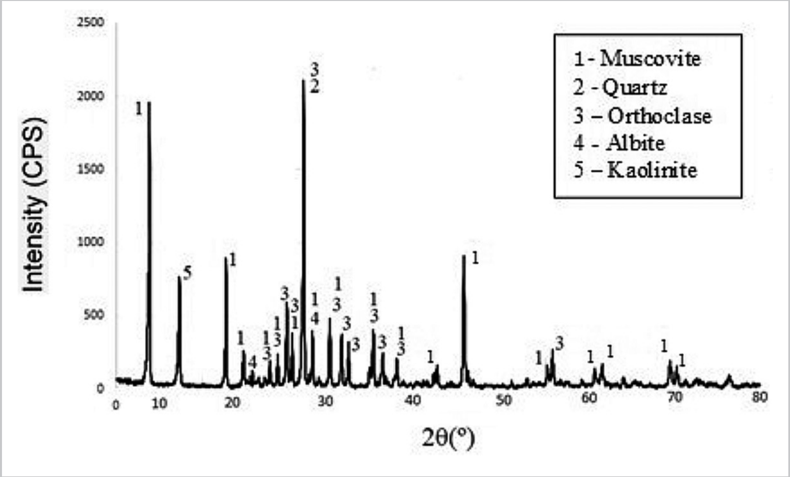

Figure 2 – K-Feldspar waste diffractogram.

Fig. 3 presents a SEM image with 32,000 times magnification of the graphene used, obtained with secondary electron detector. Fig. 4 shows two TEM images obtained according to the methodology mentioned above.

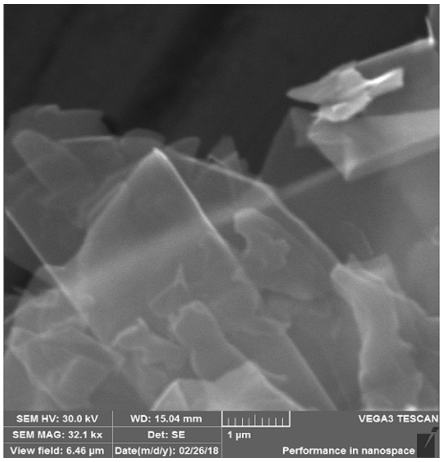

Figure 3 – SEM image of graphene used.

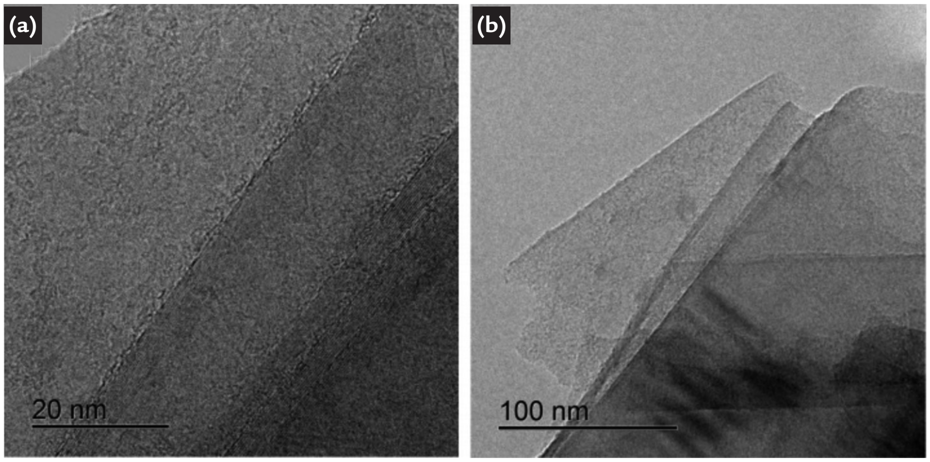

Figure 4 – TEM images of graphene used.

After performing the compressive strength test on samples without graphene and with different portions of graphene, the values obtained were as shown in Table 3 and Fig. 5 below.

Table 3 – Compressive strength values for samples without graphene and with addition of different graphene proportions.

Samples	Compressive Strength (MPa)
Sample 0%	2.02 ± 0.32
Sample 0.1%	2.08 ± 0.40
Sample 0.3%	2.79 ± 0.29
Sample 0.5%	3.32 ± 0.68

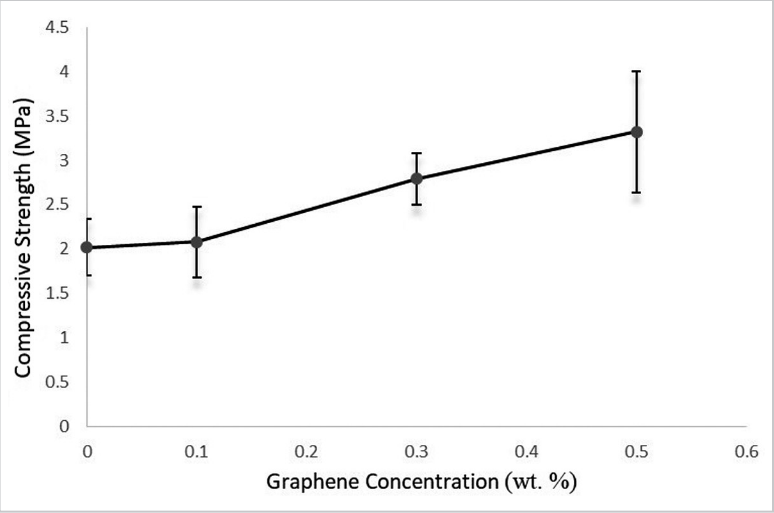

Figure 5 – Compressive Strength as a function of graphene concentration.

The diffractograms of samples with 0 wt.%; 0.1 wt.%; 0.3 wt.% and 0.5 wt.% graphene are shown below in Figures 6, 7, 8, 9, respectively. As can be seen in Fig.6, the following five phases were identified in the 0G sample: muscovite, quartz, albite, kaolinite and zeolite (hydrated aluminum and sodium silicate).

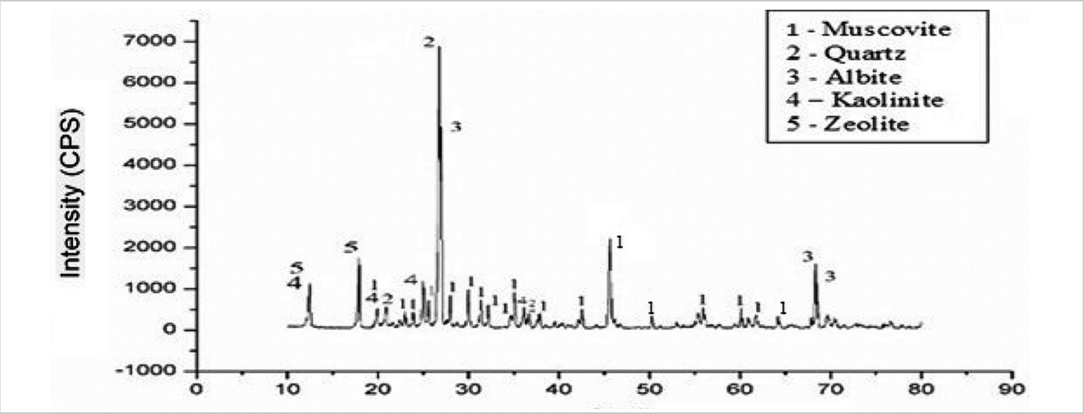

Figure 6 – Diffratogram of the sample with 0% graphene.

Notice in Figure 7, the following four phases were identified in the sample with 0.1% graphene: muscovite, quartz, kaolinite and zeolite (hydrated aluminum and sodium silicate). The respective cards in the ICDD database are: 841302, 832466, 750938 and 800700.

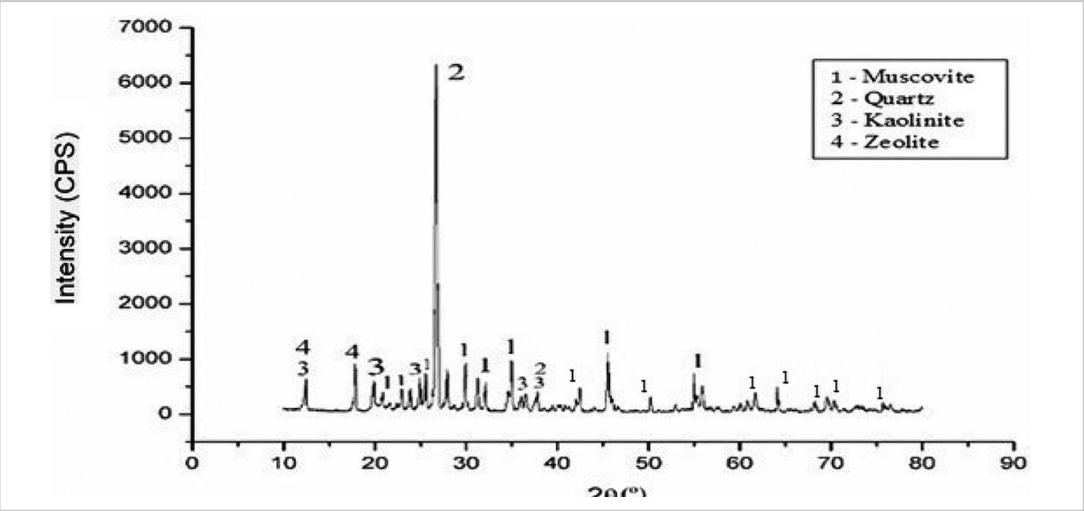

Figure 7 – Diffratogram of the sample with 0.1% graphene.

As shown in Fig.8, the following four phases were identified in the 0.3G sample: muscovite, quartz, kaolinite and zeolite (hydrated aluminum and sodium silicate). The respective cards in the ICDD database are: 841302, 832466, 750938 and 800700.

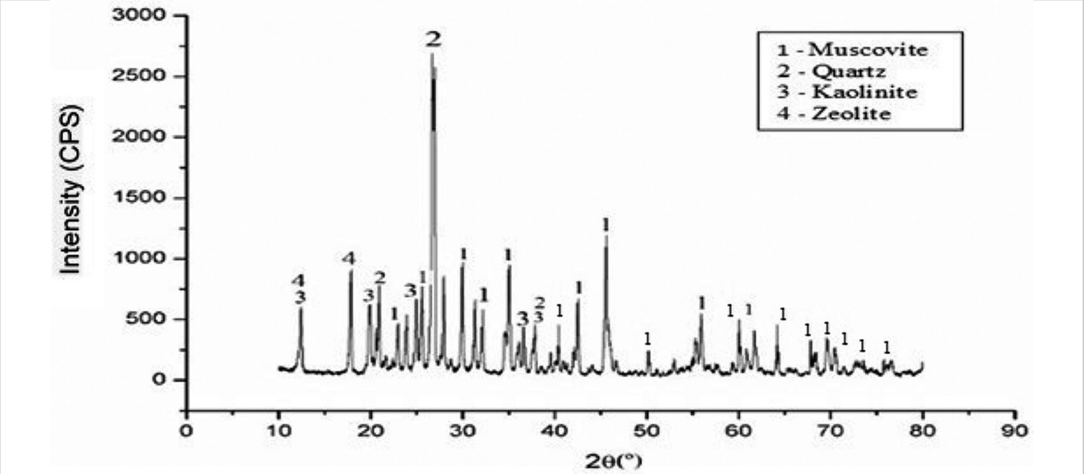

Figure 8 – Diffratogram of the sample with 0.3% graphene.

As shown in Figure 9, the following four phases were identified in the 0.5G sample: muscovite, quartz, kaolinite and zeolite (hydrated aluminum and sodium silicate). The respective cards in the ICDD database are: 841302, 832466, 750938 and 800700.

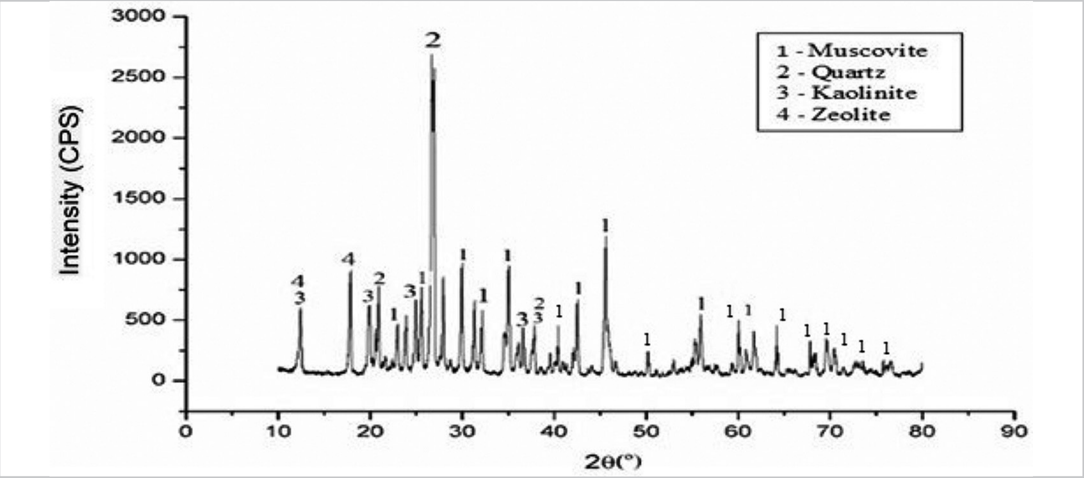

Figure 9 – Diffratogram of the sample with 0.5% graphene.

4. Discussion

The EDX result of the K-feldspar waste show the remarkable presence of the oxides Al_2O_3 and SiO_2, which, according to Yun-Ming *et al.* (2016), are primordial oxides in the manufacture of geopolymeric materials and both are in adequate proportions to justify the obtaining of cements with good mechanical properties.

Particle size measurement of the waste shows reasonably small particles. This, added to the fact that the material was sieved at 5mm and dried before being submitted to the other tests, corroborates to an efficient geopolymerization reaction and to uniform samples.

The Xpowder® software was used to analyze the diffractograms generated in the XRD analysis. As can be seen in Fig. 1, the following five phases were identified in the waste: muscovite, quartz, orthoclase, albite and kaolinite. The respective cards in the ICDD database are: 841305, 861628, 860439, 832215 and 751593. The results show the typical phases present in aluminosilicates normally submitted to successful geopolymerization reactions, as will be explained below.

In the SEM image of graphene, it is possible to observe the multi-layered graphene layers overlapping. The material consists of several overlapping thin layers. As there are very thin layers, it is noted that is possible to see the edge of the bottom layer through the center of the top layer. Therefore, the information that it is a multi-layered material is confirmed. TEM images reinforce what was observed in SEM images and allow a better visualization of the appearance of the sample, showing multiple layers of graphene. It is possible to observe in the image Fig.4b that when focusing on edges, it is possible to observe in more detail the presence of overlapping layers.

The compressive strength results with 1 day of age after curing, shown in the graph of Fig. 5 helps us to visualize the variation of the compressive strength as the graphene is added. With the addition of only 0.1 wt.% graphene, there was practically no change in strength when compared to the reference sample. However, from this sample, there is a trend of linear growth, in which an increase in strength of 0.3G in relation to 0.1G and apparently of 0.5G in relation to 0.3G is observed. However, the 0.5G sample showed a high standard deviation. The maximum increase in compressive strength achieved was 65%.

When comparing the data two by two, it showed that the 0.3G and 0.5G samples are statistically equal and there was no real increase from one sample to another, due to the fact that the standard deviation of the two samples overlap. To confirm this, an analysis of variance test (ANOVA) was performed with the values obtained for samples 0.3G and 0.5G. Values of $F = 2.5699$ and $p = 0.147576$ were obtained in the test. As $p>0.01$, it is concluded that, at a significance of 1%, there was no variation for the compressive strengths of 0.3G and 0.5G. The same comparison was performed in pairs between the reference sample and 0.3G, and between samples 0.1G and 0.3G. The results presented values of $F = 15.89544$ and $p = 0.004023$ for the first case and $F = 12.86244$ and $p = 0.007121$ for the second case, so that the result is significant at $p <0.01$ for both cases.

Therefore, it is confirmed that the graphene additions show a significant increase in the compressive strength of the samples with 0.3 wt% and 0.5 wt% of graphene. This is in accordance with the data presented by Muraleedharan and Nadir (2021), which show that the addition of nanostructured reinforcements in granite waste geopolymers contributes to higher compressive strengths, especially at early ages, as is the case in our study, in which a time of 1 day of age after curing was applied. Guo *et al.* (2020) obtained an increase around 2.9%–16.3% for compressive strength in graphene reinforced geopolymers. The authors promoted the study in furnace slag and fly-ash based geopolymers.

The raw materials used had a D-average particle size equivalent to 13.73 and 9.68 respectively. Considering the waste used in this study, they presented a D-average of 9.65, and it is observed that the increases in compressive strength obtained were satisfactory.

Ranjbar *et al.* (2015) performed a study on fly-ash based geopolymers reinforced with graphene nanoplatelets. The highest compressive strength was improved by 1.44 times with the 1 wt.% graphene addition. As noted by the authors, it is possible to achieve higher increases in compressive strength with greater additions of graphene. However, in this situation, it is necessary to obtain a good dispersion of graphene in the geopolymer matrix since the existence of overlapped graphene nanoplatelets or the agglomeration in particular regions are defective and result in nullifying the additional strength.

For subsequent research, it is suggested to carry out tests with graphene concentrations higher than 0.5 wt.%; in order to verify the maximum value of the graphene concentration that promotes increases in the mechanical strength of the material.

As shown by Fragas *et al.* (2016), the compressive strength of the manufactured geopolymeric specimens are similar to that which is expected for mortars used in non-structural masonry, applicable in auxiliary structures. It is worth considering that Fragas *et al.* (2016) studies a Portland cement mortar, which, differently from the geopolymeric material of our study, presents different curing times and reactions, but it is possible to make a comparison in terms of compressive strength only, considering that both are meant for the same application.

The diffratogram of the reference geopolimeric sample is shown in Fig. 6. The respective cards in the ICDD database are: 841302, 832466, 030451, 750938 and 800700. It is observed that, in comparison with the waste sample before geopolymerization, the muscovite, quartz, albite and kaolinite phases are repeated. The main change is in the absence of the orthoclase phase, which is a feldspar mineral, and in the appearance of a hydrated aluminum and sodium silicate, from the zeolite family. The appearance of such a phase would be evidence of the process of geopolymerization, since, according to Bumanis *et al.* (2017), geopolymers would be constituted by a sodium aluminosilicate hydrate, zeolite type phase, which would even justify the effectiveness of using these materials in applications involving ion exchange, as water treatment for example.

Provis, Lukey and van Deventer (2005) explain that part of the bonding phase formed in geopolymerization is composed of nanometric crystalline structures, which resemble the nucleus in which the zeolites crystallize. The agglomeration of these nanocrystallites by the remaining aluminosilicate material, in the form of a gel, forms a high-performance mineral binder, commonly referred to as geopolymer or alkali-activated material. The presence of the sodium aluminosilicate hydrate phase in these materials and the direct correlation with the occurrence of a successful alkali-activation reaction and increased mechanical strength was also observed by Rakngan *et al.* (2018); Walkley *et al.* (2018); Myers, Bernal and Provis (2017); Ridha *et al.* (2018) and Xiao *et al.* (2020).

It is noted that as the graphene content in the sample increases, the main peak of the quartz sample decays considerably, from approximately 7,000 cps in the sample with 0% graphene to 2,500cps in in the sample with 0.5 wt.% graphene. This is due to the fact that the formation of a solid solution possibly occurred, resulting in decreased peak intensity while maintaining the peak area, probably indicates a decrease in the crystallite size. Takeda (2013) studies the effect of crystallite size on a zeolite-based geopolymer strength and notes that the crystallite size and strength are inversely proportional, which would explain the change in crystallite size provided by graphene as the cause of the increase in material strength.

5. Conclusions

It was possible to perform the geopolymerization of the waste from the extraction of K-feldspar. The mechanical strength values achieved place the material as a potential geopolymeric mortar, for applications in non-structural masonry. The addition of graphene into the material promoted increases in its compressive strength to values greater than 0.1 wt.% of added graphene. The maximum value of increase in strength obtained was 65% in relation to the reference sample. This behavior shows that very low additions of graphene can promote disruptive effects on the mechanical strength of the material.

Currently, searches have been ceaseless for cheap raw materials with ecological appeal that result in products with good mechanical properties and good performance in the field. The study of the reuse of waste places this study in line with the environmental concerns raised in recent years due to catastrophes that occurred with tailings dams in Minas Gerais state, Brazil. Thus, the use of K-feldspar mining waste as a precursor for the manufacture of geopolymeric mortar, as shown by the results, is a promising technology that fulfils the ecological demands of the current market.

Furthermore, in line with the most modern technological trends, graphene comes as a powerful tool of nanotechnology to allow the manufacture of materials with remarkable properties, as well as products with satisfactory performance but savings in raw materials, adding only minimal percentages of graphene. It is concluded that the studied waste can be applied as a mortar in non-structural masonry using the geopolymerization technique and that multi-layered graphene can be used to promote increases in the mechanical strength of the material produced.

Acknowledgments

This work was carried out thanks to a partnership between CEFET-MG and the company Phosther Tecnologia de Aglomerações. The research was funded by Phosther in order to test other possible applications for the materials they produce.

References

ARAUJO, M. M. S.; SANTOS, H. I.; FERREIRA, O. M. ***Análise do gerenciamento dos resíduos sólidos da mineração Serra Grande S.A., Município de Crixás - Goiás.*** 2012. 180 f. Trabalho de Conclusão de Curso (Bacharelado em Engenharia Ambiental) – Faculdade de Engenharia, Pontifícia Universidade Católica de Goiás, Goiânia, 2012.

ARIOZ, E.; ARIOZ, Ö; KOÇKAR, M. The effect of curing conditions on the properties of geopolymer samples. ***International Journal of Chemichal Engineering and Applications***, v. 4, n. 6, p. 423–426, 2014.

ASSOCIAÇÃO BRASILEIRA DE NORMAS TÉCNICAS. ***ABNT NBR 16697***: Cimento Portland - Requisitos.

Rio de Janeiro: ABNT, 2018.

BUMANIS, G.; VITOLA, L.; FERNANDES-JIMENEZ, A.; PALOMO, A.; BAJARE, D. The effect of heat treatment in alkali activated materials. ***Ceramics and Glasses***, v. 23, n. 3, 2017.

FRAGAS, T.; MACIEL, L; COELHO, A.; PEREIRA, H. R. S. Análise comparativa da determinação da resistência à compressão em argamassas com pó de pedra em substituição parcial à areia natural. In: Congresso Brasileiro de Cerâmica, 60., 2016, Águas de Lindóia. ***Anais*** [...]. Águas de Lindóia: ABCERAM, 2016. p. 830-839.

GOMES, A. C. F. ***Estudo de aproveitamento de rejeito de mineração***. 2017. 98 f. Dissertação (Mestrado em Engenharia Metalúrgica, Materiais e de Minas) - Universidade Federal de Minas Gerais, Belo Horizonte, 2017.

GUO, S.; QIAO, X.; ZHAO, T.; WANG, Y.-S. Preparation of highly dispersed graphene and its effect on the mechanical properties and microstructures of geopolymers. ***Journal of Materials in Civil Engineering***, v. 32, n. 11, 2020.

MEHTA, A.; SIDDIQUE, R. An overview of geopolymers derived from industrial by-products. ***Construction and Building Materials***, v. 127, p. 183-198, 2016.

MENDONÇA, V. M. ***Adição de grafeno a argamassas geopoliméricas desenvolvidas a partir de resíduo da mineração de feldspato potássico***. 2020. 86 f. Dissertação (Mestrado em Engenharia de Materiais) – Centro Federal de Educação Tecnológica de Minas Gerais, Belo Horizonte, 2020. Available at: https://www.cefetmg.br/wp-content/uploads/2020/09/Disserta%C3%A7%C3%A3o-Defesa-Vin%C3%ADcius-Meirelles-Mendon%C3%A7a--versao-final.pdf. Accessed: 08 mar. 2020.

MURALEEDHARAN, M.; NADIR, Y. Factors affecting the mechanical properties and microstructure of geopolymers from red mud and granite waste powder: a review. ***Ceramics International***, v. 47, n. 10, p. 13257–13279, May 2021. Available at: https://doi.org/10.1016/j.ceramint.2021.02.009. Accessed: 09 mar. 2020.

MYERS, J.; BERNAL, S. A.; PROVIS, J. L. Phase diagrams for alkali-activated slag binders. ***Cement and Concrete Research***, v. 95, p. 30-38, 2017.

PROVIS, J. L.; LUKEY, G. C.; VAN DEVENTER, Jannie S. J. Do geopolymers actually contain nanocrystalline zeolites? A reexamination of existing results. ***Chemistry of Materials***, v. 17, n. 12, p. 3075-3085, 2005.

RAKNGAN, W.; WILLIAMSON, T.; FERRON, R. D.; SANT, G.; JUENGER, M. C. G. Controlling workability in alkali-activated Class C fly ash. ***Construction and Building Materials***, v. 183, p. 226-233, 2018.

RANJBAR, N.; MEHRALI, M.; ALENGARAM, U. J.; JUMAAT, M. Z. Graphene nanoplatelet-fly ash based geopolymer composites. ***Cement and Concrete Research***, v. 76, p. 222-231, 2015.

RIDHA, S.; SETIAWAN, R. A.; ABD HAMID, A. I.; SHAHARI, A. R. The influence of CO_2 accelerated carbonation on alkali-activated fly ash cement under elevated temperature and pressure. ***Materials Science and Engineering Technology***, v. 49, n.44, p. 483-488, 2018.

SINGH, B.; ISHWARYA, G.; GUPTA, M.; BHATTACHARYYA, S. K. Geopolymer concrete: a review of some recent developments. ***Construction and Building Materials***, v. 85, p. 78-90, 2015.

TAKEDA, H.; HASHIMOTO, S.; YOKOHAMA, H.; HONDA, S.; IWAMOTO, Y. Characterization of zeolite in zeolite-geopolymer hybrid bulk materials derived from kaolinitic clays. ***Materials***, v.6, n.5, 1767-1778, 2013.

TURNER, L. K.; COLLINS, F. G. Carbon dioxide equivalent (CO2-e) emissions: A comparison between geopolymer and OPC cement concrete. ***Construction and Building Materials***, v. 43, p. 125-130, 2013.

WALKLEY, B.; KASHANI, A.; MARC-ANTOINE, S.; NGO, T. D.; MENDIS, P. Examination of alkali-activated material nanostructure during thermal treatment. ***Journal of Materials Science***, v. 53, n.13 p. 9486-9503, 2018.

XIAO, R.; JIANG, X.; ZHANG, M.; POLACZYK, P.; HUANG, B. Analytical investigation of phase assemblages of alkali-activated materials in CaO-SiO2-Al2O3 systems: the management of reaction products and designing of precursors. ***Materials & Design***, v.194, 2020.

YAN, S.; HE, P.; JIA, D.; YANG, Z.; DUAN, X.; WANG, S.; ZHOU, Y. In situ fabrication and characterization of graphene/geopolymer composites. ***Ceramics International***, v.41, p. 11242-11250, 2015.

YUN-MING, L.; CHENG-YONG, H.; AL BAKRI, M. M.; HUSSIN, K. Structure and properties of clay-based geopolymer cements: a review. ***Progress in Materials Science***, v. 83, p. 595-629, 2016.

Received: 4 March 2020 - Accepted: 29 April 2021.